PHYSICAL REVIEW B **71**, 174404 (2005)

Antiferromagnetic transitions in polymorphous minerals of the natural cuprates atacamite and botallackite $Cu_2Cl(OH)_3$

X. G. Zheng,[1,*] Takashi Mori,[1] Kusuo Nishiyama,[2] Wataru Higemoto,[2] Hiroshi Yamada,[3] Keiko Nishikubo,[4] and C. N. Xu[3,4]

[1]*Department of Physics, Saga University, Saga 840-8502, Japan*

[2]*Meson Science Laboratory, Institute of Material Structure Science, High Energy Accelerator Research Organization (KEK-MSL), Ibaraki 305-0801, Japan*

[3]*PRESTO, Japan Science and Technology Corporation (JST), Honcho, Kawaguchi, Saitama 332-0012, Japan*

[4]*National Institute of Advanced Industrial Science and Technology, Tosu, Saga 841-0052, Japan*

(Received 28 June 2004; revised manuscript received 10 December 2004; published 5 May 2005)

A systematic study on pure-phase samples of the polymorphous natural cuprates $Cu_2Cl(OH)_3$, atacamite and botallackite, is carried out using synchrotron x-ray-diffraction, magnetic susceptibility, and muon spin rotation/relaxation (μSR) measurements. Atacamite and botallackite are found to undergo antiferromagnetic transition at $T_N=9.0$ and $T_N=7.2$ K, respectively. Contrasting results are obtained in the μSR. Atacamite is suggested to have a distribution in the internal (electron-spin) field, favoring a picture of a disordered ground state, while botallackite shows distinct muon-spin rotation, indicating a long-range magnetic order. The different magnetic properties exhibited by the two polymorphs are consistently explained by inspection into the coordination of Cu and the Cu-O-Cu bond angles in the polymorphs.

DOI: 10.1103/PhysRevB.71.174404 PACS number(s): 75.90.+w, 76.75.+i, 91.60.Pn, 75.50.−y

I. INTRODUCTION

Minerals $Cu_2Cl(OH)_3$ are known to exist in polymorphs, i.e., atacamite in orthorhombic ($a=6.030$ Å, $b=6.865$ Å, $c=9.120$ Å), botallackite in monoclinic ($a=5.715$ Å, $b=6.124$ Å, $c=5.632$ Å, $\beta=92.75$), the newly identified clinoatacamite in monoclinic ($a=6.157$ Å, $b=6.814$ Å, $c=9.104$ Å, $\beta=99.65$), and possibly a metastable paratacamite in rhombohedral ($a=13.654$ Å, $c=14.041$ Å, replacement of Cu by small amounts of another cation is necessary to stabilize the paratacamite structure), respectively.[1–5] The $Cu_2Cl(OH)_3$ are sometimes called natural cuprates in the meaning that they contain copper-oxygen bonds. We consider that it is of interest to compare their magnetic properties with those of the artificial high-T_c superconducting cuprates, especially because the magnetic interaction between the Cu^{2+} spins in the high-T_c superconducting cuprates is believed an essential factor for the high-T_c superconductivity.

The research of $Cu_2Cl(OH)_3$ is interesting itself because the correlation between the crystal structure and their physical properties can be directly shown by the different properties exhibited by the polymorphs. The magnetic properties of the differently structured $Cu_2Cl(OH)_3$ polymorphs are not clear. For example, a spin-glass behavior was previously reported for synthetic atacamite, while mineral atacamite apparently showed antiferromagnetic behavior.[6,7]

Another motivation of the present research arises from a recent topic. Recently an organic/inorganic hybrid system $Cu_2X(OH)_3$ (X=carboxylate) receives much attention by showing antiferromagnetic and weak ferromagnetic behaviors as well as glassiness in different samples.[8,9] The different magnetic properties are attributed to slight difference in the Cu-O-Cu coordination that is influenced by the exchangeable anion X, a phenomenon named "solvato-magnetism."[10] The $Cu_2X(OH)_3$ samples were reported to exhibit botallackite structure and triangular quantum Heisenberg antiferromagnetic lattice is proposed. Deuterium NMR studies on $Cu_2X(OD)_3$ ($X=NO_3, HCOO, C_6H_5COO$) showed varied exchange interactions of $J=+19(11)$ and $-21(3)$ K for $X=NO_3$, $J=+13(7)$ and $-13(5)$ K for X=HCOO, and $J=-54(4)$ and $-92(3)$ K for $X=C_6H_5COO$, respectively.[11,12] Unfortunately, the fine crystal structures of the $Cu_2X(OH)_3$ with large X have not been solved due to their unsatisfactory crystallization.[13] In order to reveal the magnetic mechanism, μSR studies (the longitudinal field decoupling and muon-spin resonance) have been carried out for small inorganic anions X (X=Cl, I). Three muon sites were suggested for $Cu_2Cl(OH)_3$, while two were observed for $Cu_2I(OH)_3$. Since the muon is considered to stop at the same sites in these salts, the authors concluded that the Cl and I salts have different magnetic structures by assuming an additional ferromagnetic coupling in $Cu_2Cl(OH)_3$.[14] However, our recent experience on the $Cu_2Cl(OH)_3$ polymorphs clearly show that sample characterization is of vital importance for the $Cu_2Cl(OH)_3$ system since the synthesis of one of the polymorphs usually was accompanied by the formation of other impurity polymorphous phases. As a matter of fact, we had observed weak ferromagnetic and antiferromagnetic behaviors, as well as glassiness, with the different phases. Therefore, a detailed research on the respective $Cu_2Cl(OH)_3$ polymorphs is demanded.

The present work reports the results of magnetic susceptibility and muon-spin relaxation (μSR) measurements on single-phase atacamite and botallackite. The present study reveals that atacamite and botallackite are antiferromagnets with different T_NS and magnetic structures.

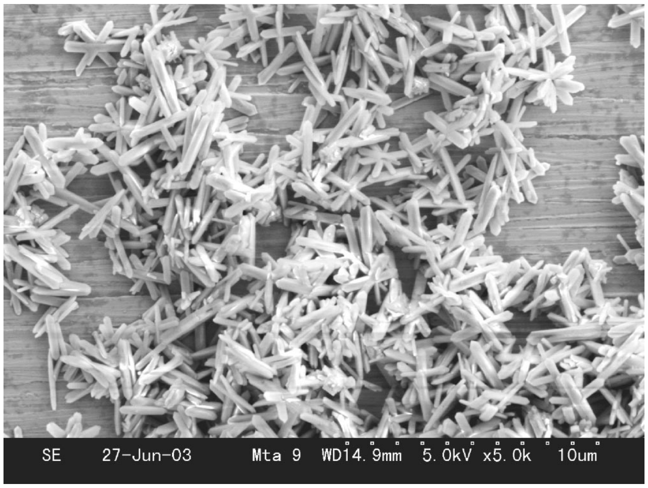

FIG. 1. Field-emission scanning electron microscopy for botallackite.

II. EXPERIMENTAL

Pure-phase atacamite and botallackite were synthesized, respectively, from solution reaction of cupric formate tetrahydrate and potassium chloride by adjusting the temperature and solution concentration. For atacamite, minerals as natural products in small (~millimeter) crystalline form (mined from Arizona) are available. Since our synthesized pure atacamite showed the same crystal structures and magnetic susceptibility behaviors as the mineral (but poorer crystal nature), we used the mineral crystals in the present report. The synthesized botallackite are good micro crystals (~1 μm) as shown in Fig. 1. The two compounds were characterized using synchrotron x-ray diffraction at Spring-8, BL02B2. This beamline is designed for accurate structure analysis with powder samples using a Debye-Scherrer camera with an imaging plate. The incident x-ray was monochromatized by a double-crystal monochromator tuned to the wavelength of 0.5 Å. All powder diffraction data were analyzed by the Rietveld technique, using the RIETAN-2000 program.[15] The temperature dependence of the dc susceptibility was measured using a commercial SQUID magnetometer. Zero-field (ZF) and longitudinal-field (LF) muon-spin rotation/relaxation (μSR) were carried out at Meson Science Laboratory, High Energy Accelerator Research Organization (KEK-MSL) by using a pulsed (20 ns/bin) surface μ^+ beam with energy of 4 MeV, then repeated at the TRIUMF M20 channel by using a continuous surface μ^+ beam (0.4 ns/bin) to see muon-spin rotations. The ZF-μSR was carried out in a field less than 1 mOe. The asymmetry parameter of the muon spin at time t, $a(t)$, is defined as $[F(t)-B(t)]/[F(t)+B(t)]$, where $F(t)$ and $B(t)$ are muon events counted by the forward and backward counters, respectively. The incident muons are polarized along the longitudinal progressing direction and the initially polarized muons are depolarized by the internal fields in the specimen. Therefore, magnetic transition can be directly witnessed in the muon spectra.

III. RESULTS AND DISCUSSION

A. Material characterization

In Figs. 2 and 3 the observed and calculated x-ray-diffraction patterns for atacamite and botallackite are shown respectively. Out of the measured range of 2.5–75°, only the data from 4° to 15° are shown for a clear view. The detailed information about the structures is summarized in Tables I and II, respectively, for atacamite and botallackite. The structures are in good agreement with those previously determined by normal x-ray diffractions on single crystals of mineral atacamite and botallackite (1, 4). To show the coordination of the atoms and the features of the structure, the structures are illustrated in Figs. 4 and 5, respectively, for atacamite and botallackite. Atacamite is featured by Cu-O-Cu chains running along the *b* axis with the chains connected by CuO ladders in the *a*-axis direction. Botallackite is featured by CuO chains along the *a* axis with the chains intersecting with CuO_2 ladders along the *c* axis. A strong feature in botallackite is that the CuO planes, consisting of the ladders and chains, are stacking in a layered structure as viewed from the *b* axis in Fig. 5. As is seen in the figures and tables, differences are seen in the Cu-O-Cu bond angles between the two structures. In atacamite the bond angles vary from 97° to 124°, while in botallackite they are in a narrow range of 101°–108°.

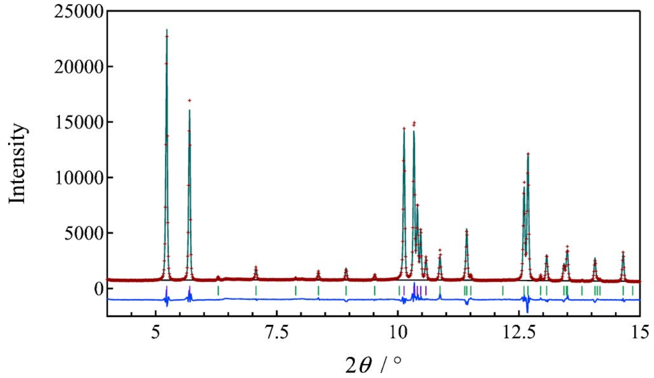

FIG. 2. (Color online) Observed and calculated synchrotron x-ray-diffraction spectra for atacamite.

B. Magnetic susceptibility

The temperature dependences of the susceptibility for the two structures are shown in Fig. 6. Maximums at 9.0 K and

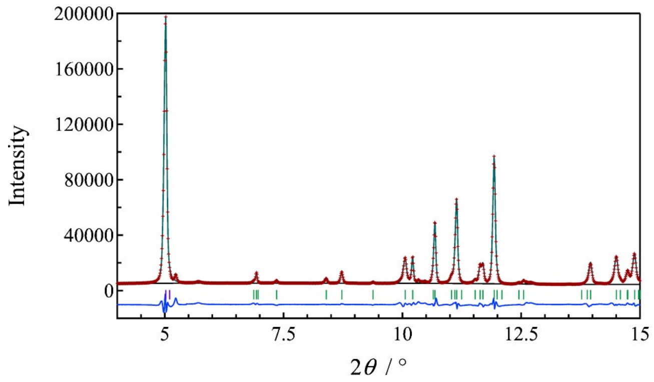

FIG. 3. (Color online) Observed and calculated synchrotron x-ray-diffraction spectra for botallackite.

TABLE I. Structure information for atacamite.

Compound name	Atacamite
Chemical formula	$Cu_2Cl(OH)_3$
Cell setting	Orthorhombic
Space group	*Pnma* (no. 62)
Z	4
a (Å)	6.02797(11)
b (Å)	6.86383(13)
c (Å)	9.11562(17)
V (Å^3)	377.158(12)
D (gcm^{-3})	3.76
$R_{wp}(S)$	0.0452 (1.2571)
R_B	0.0635

$^a S=R_{wp}/R_e$

Atom	Site	g	x	Y	z	U (10^{-2} Å^2)
Cu1	4*a*	1	0	0	0	0.80(3)
Cu2	4*c*	1	0.19257(17)	1/4	0.25603(17)	0.86(4)
Cl	4*c*	1	0.3514(4)	3/4	0.0565(3)	1.33(7)
O1	4*c*	1	0.1498(8)	1/4	−0.0069(7)	0.66(14)
O2	8*d*	1	0.4394(6)	0.0636(5)	0.2875(4)	0.67(10)
H1	4*c*	1	0.585(12)	3/4	0.059(8)	0.66
H2	8*d*	1	0.389(8)	0.579(6)	0.133(6)	0.66

Bond length (Å)		Bond angle (°)	
Cu1-O1	1.940(2)	Cu1-O1-Cu1^{ii}	124.392(2)
Cu1-O2^{i}	2.019(3)	Cu1-O2^{i}-Cu2	100.830
		Cu2-O2-Cu2^{iii}	97.4(2)
Cu2-O2	1.984(3)	Cu2^{iii}-O2^{iv}-Cu1^{v}	114.462
Cu2-O2^{i}	2.031(3)		

Symmetry codes: (i) $x-1/2$, y, $1/2-z$; (ii) $-x$, $y+1/2$, $-z$; (iii) $x+1/2$, $1/2-y$, $1/2-z$; (iv) $x+1/2$, $1/2-y$, $1/2-z$; (v) $1-x$, $y+1/2$, $-z$

7.2 K were observed for atacamite and botallackite, respectively, suggesting that atacamite and botallackite undergo antiferromagnetic transitions below $T_N=9.0$ K and 7.2 K, respectively. In atacamite, the reciprocal susceptibility does not change linearly with the temperature (Fig. 7). We also found the same susceptibilities with synthesized atacamite. Since the synthesized atacamite and the mineral showed same susceptibilities and the XRD shows a single phase for both samples, we conclude that the results in Fig. 7 suggest multiple magnetic exchange interaction J values, and possibly frustration. The observed susceptibilities of botallackite obey Curie-Weiss law $1/\chi=C/(T-\theta)$ in the whole temperature range above T_N: the Curie-Weiss constants were determined to be $C=0.76$ emu K mol^{-1} and $\theta=0.41$ K.

C. Muon-spin rotation and relaxation

The magnetic transtion was ambiguously verified by the μSR measurements. In Figs. 8 and 9 the ZF-μSR spectra for atacamite and botallackite, respectively, are presented. In the paramagnetic state the depolarization behavior is well described by the Kubo-Toyabe function[16]

$$a(t)=\frac{1}{3}+\frac{2}{3}(1-\sigma^2t^2)\exp\left[-\left(\frac{1}{2}\right)\sigma^2t^2\right] \tag{1}$$

due to the nuclear field of Cu63 or Cu65 (where 1/3 of the muon spins remain the initial longitudinal direction and 2/3 muon spins rotate and depolarize due to the other two vertical components of the field). Relaxation of electron spin is too fast to depolarize muon spin at this temperature. In our experiment, an equivalent $\sigma=0.44$ μs^{-1} was observed for atacamite and botallackite in the paramagnetic state. It is consistent with the previous study by Maruta *et al.*, who reported the Kubo-Toyabe type relaxation with a same $\sigma=0.43$ μs^{-1} for $Cu_2X(OH)_3$ ($X=$Cl, Br, I) regardless of the halide ions.[14] Therefore, it is clear that muon stops around hydroxyl ion rather than halide ion in this system to produce the waterlike molecule: $\mu^+ + OH^- \rightarrow MuOH$. Thus muon serves as a probe for the local magnetic field that is caused by electron spin at oxygen site. When a magnetic order is developed inside the specimen, static internal field is pro-

TABLE II. Structure information for botallackite.

Compound name	Botallackite
Chemical formula	$Cu_2Cl(OH)_3$
Cell setting	Monoclinic
Space group	$P2_1/m$ (no. 11)
Z	2
a (Å)	5.7165(3)
b (Å)	6.1182(3)
c (Å)	5.6283(2)
β (°)	93.1161(14)
V (Å^3)	196.556(16)
D (gcm^{-3})	3.61
$R_{\mathrm{wp}}(S)$	0.0393 (2.88)
R_{B}	0.0304

[a] $S = R_{\mathrm{wp}}/R_{\mathrm{e}}$

Atom	Site	g	x	y	z	U (10^{-2} Å^2)
Cu1	$2e$	1	0.4897(4)	1/4	0.9980(4)	0.80(3)
Cu2	$2d$	1	1/2	1/2	1/2	0.80
Cl	$2e$	1	0.1319(5)	1/4	0.2954(5)	1.69(8)
O1	$2e$	1	0.3261(12)	3/4	0.3714(11)	0.88(8)
O2	$4f$	1	0.3617(7)	0.5079(10)	0.8187(7)	0.88
H1	$2e$	1	0.946(17)	1/4	0.536(14)	1.6
H2	$4f$	1	0.246(9)	0.831(9)	0.979(9)	1.6

Bond length (Å)		Bond angle (°)	
Cu1-O2	1.991(5)	Cu2-O1-Cu2$^{\mathrm{ii}}$	103.876
Cu1-O2$^{\mathrm{i}}$	1.971(5)	Cu2-O2-Cu1	106.450
Cu2-O1	1.943(4)	Cu2-O2-Cu1$^{\mathrm{iii}}$	107.908
Cu2-O2	2.000(4)	Cu1-O2-Cu1$^{\mathrm{iii}}$	101.2(2)

Symmetry codes: (i) $1-x$, $1-y$, $2-z$; (ii) $1-x$, $y+1/2$, $1-z$; (iii) $1-x$, $y+1/2$, $2-z$.

duced by the ordered spins, and the asymmetry rapidly decreases toward a time-independent baseline of 1/3. If the magnetic order is long range and the sample is crystalline, then oscillation around the baseline can be seen with the high time resolution of a continuous beam.

Magnetic transition around 9 K in atacamite and that between 7 and 7.5 K in botallackite are seen, respectively, in the depolarization behaviors in Figs. 8 and 9. The development of a long-range order in botallackite is further directly witnessed in the high-resolution asymmetry spectra obtained with the continuous beam at TRIUMF. Distinct rotations with well-defined frequencies of 8.7 and 21.9 MHz at 2.1 K, which correspond to two stop sites, are seen for botallackite (Fig. 10). The phase diagram by plotting the muon-spin rotation frequencies to temperature (Fig. 11) agrees with the antiferromagnetic transition at $T_N = 7.2$ K as seen in the susceptibility. The muon-spin frequencies are also consistent with the result of our LF-μSR experiment on botallackite.

On the other hand, no distinct muon spin rotation was seen in atacamite even with the continuous beam. In the ordered phase, when a longitudinal field is applied to the specimen, the depolarized muon spins are decoupled and the average magnitude of the internal static field felt by the muons can be roughly estimated from the decoupling behavior

$$P = \frac{3}{4} - \frac{1}{4x^2} + \frac{(x^2-1)^2}{16x^2} \log \frac{(x+1)^2}{(x-1)^2}, \tag{2}$$

where $x = H_{\mathrm{LF}}/H_{\mathrm{local}}$, H_{LF} is the external field parallel to the initial muon polarization and H_{local} the local field. Therefore, we can estimate the average internal field in atacamite. The fitting of the LF-μSR in Fig. 12 to one muon site give an average internal field of ~320 (40) Oe for atacamite. As will be described in detail below, the ZF-μSR of atacamite at 2 K is characterized by a quick exponential dive around 0.2 μs and recovery around 0.5 μs, thereafter a slow Gaussian decrease. The asymmetry at the recovery is nearly 1/3 of the paramagnetic asymmetry, and the recovered values of the asymmetries were used for the LF-μSR fit. A previous experiment reported three sites with local fields of 39 (130), 320 (90), and 840 (130) Oe for synthetic botallackite.[14] The value of 320 Oe is considered due to inclusion of atacamite phase in their specimen.

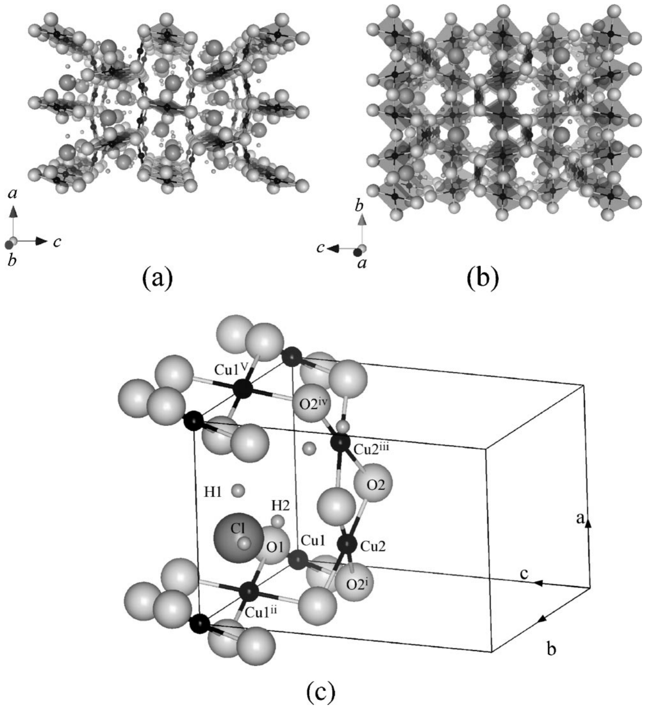

FIG. 4. Crystal structure of atacamite $Cu_2Cl(OH)_3$; (a) viewed from *b* axis, (b) viewed from *c* axis, and (c) local coordination.

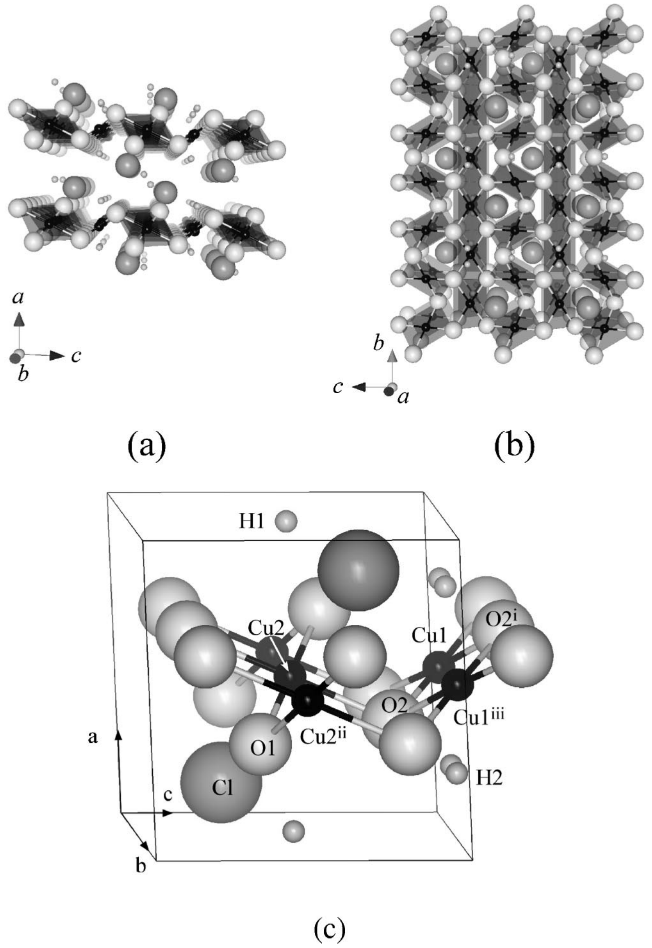

FIG. 5. Crystal structure of botallackite $Cu_2Cl(OH)_3$; (a) viewed from *b* axis, (b) viewed from *a* axis, and (c) local coordination.

The transition in atacamite can be more clearly seen by analyzing the ZF-μSR spectra. In an antiferrimagnet the depolarization close to the magnetic transition usually can be described by a combination of an exponential function with the Kubo-Toyabe function, i.e.,

$$a(t) = a(0)\exp(-\lambda t)\left[\frac{1}{3}+\frac{2}{3}(1-\sigma^2t^2)\right]\exp\left(-\left(\frac{1}{2}\right)\sigma^2t^2\right), \tag{3}$$

where the exponential function expresses the depolarization due to the fluctuation of the magnetic field caused by the Cu^{2+} spins. However, this is not the case in atacamite. The ZF-μSR spectra of atacamite cannot be fitted by a simple exponential function. Instead it is best fitted by a combined function of

$$\begin{aligned} a(t) &= a_1\left[\frac{1}{3}+\frac{2}{3}(1-\lambda t)\exp(-\lambda t)\right] \\ &\quad + a_2\left[\frac{1}{3}+\frac{2}{3}(1-\sigma^2t^2)\exp\left(-\frac{1}{2}\sigma^2t^2\right)\right], \end{aligned} \tag{4}$$

where the former function expresses depolarization due to internal static fields with a Lorentzian distribution. Therefore, transition into magnetic order is witnessed by the increase (decrease) in a_1 (a_2) as well as the rise in λ, as is seen in Fig. 13. The fitting to the present function suggests a disordered ground state in atacamite.

It is noted that in Fig. 13 even at the lowest temperature, a part of the muons ($\sim$14%) remained paramagnetic, as is more clearly seen by the LF-μSR in Fig. 12. The depolarization due to the paramagnetic field is completely decoupled by a weak field of 100 Oe. Although the specimen is natural mineral (which means it might contain some impurities), the XRD spectra did not show a noticeable impurity phase and synthetic atacamite showed equivalent magnetic susceptibilities as the mineral sample, we think that the 14% component is intrinsic in atacamite. In an antiferromagnet, if the muons stop by a site where the static fields due to the antiparallel spins are just cancelled, then a part of the muons would show paramagnetic behavior. It is possible that there are muon site(s) in atacamite where the static field is canceled.

D. Discussion

Combing the results of the magnetic susceptibility and μSR, it is clearly seen that atacamite and botallackite undergo antiferromagnetic transitions at 9.0 K and 7.2 K, respectively. Botallackite clearly shows a long-range antiferromagnetic order, while atacamite favors a picture of disordered ground state. The disorder might enhance in a synthetic atacamite because of enhanced randomness, which seems not in conflict with the previously reported spin-glass-like susceptibility behaviors for low-temperature grown synthetic atacamite.[6] We learned from our experiments that the synthesis of one of the $Cu_2Cl(OH)_3$ polymorphs is often accompanied by another one. An independent experiment on

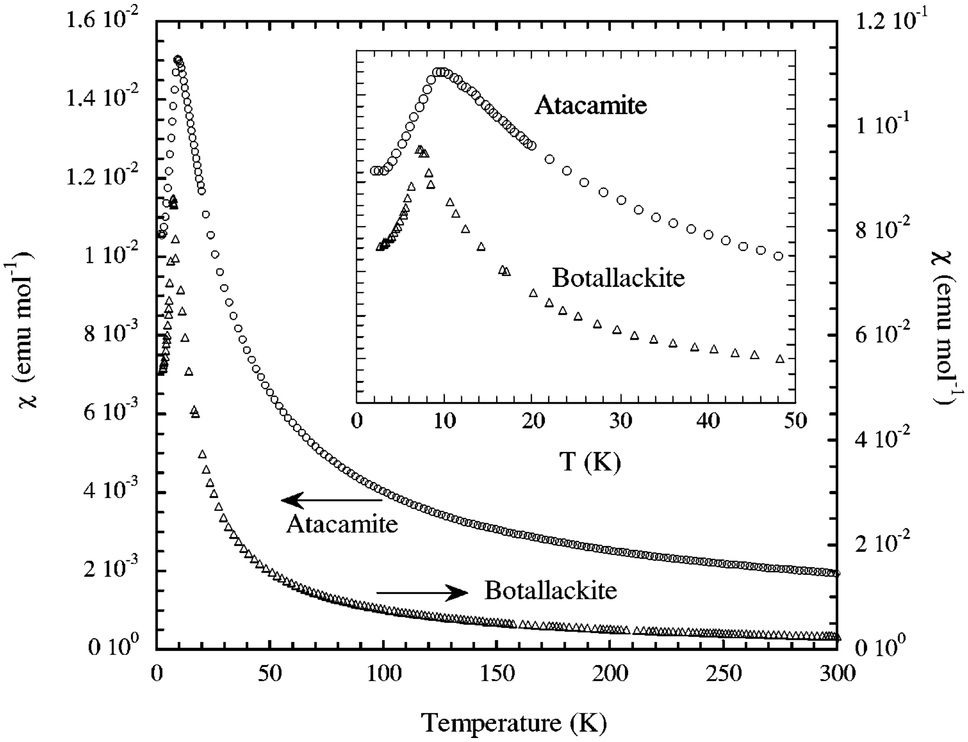

FIG. 6. Temperature dependence of the magnetic susceptibility at 10 kOe for atacamite and botallackite.

clinoatacamite shows that another polymorph of clinoatacamite shows weak ferromagnetism and glassiness.[17] As is seen from the different magnetic behaviors in the $Cu_2Cl(OH)_3$ polymorph, we think that great attention should be paid to the sample characterization in discussing the phenomenon of "solvato-magnetism" in the $Cu_2X(OH)_3$ system.

It is interesting to compare the two polymorphous compounds of atacamite and botallackite in view of the correlation between the crystal structure and the magnetic coupling. The Cu-Cl bonds are much longer than those of Cu-O in atacamite and botallackite, thus the superexchange coupling can be assumed to be primly through the Cu-O-Cu bonds. An inspection to the Cu-O bond lengths and Cu-O-Cu angles in Tables I and II reveal that the superexchange coupling in atacamite would be preferred along the $Cu1$-$O1$-$Cu1^{ii}$, which has the shortest bond and largest angle of 124.39°. However, exchange couplings, and possibly even ferromagnetic coupling, in other directions are also possible. In atacamite the bond angles vary from 97° to 124° with nearly constant bond lengths, therefore, multiple interactions with different *J*s can be in action which produce the

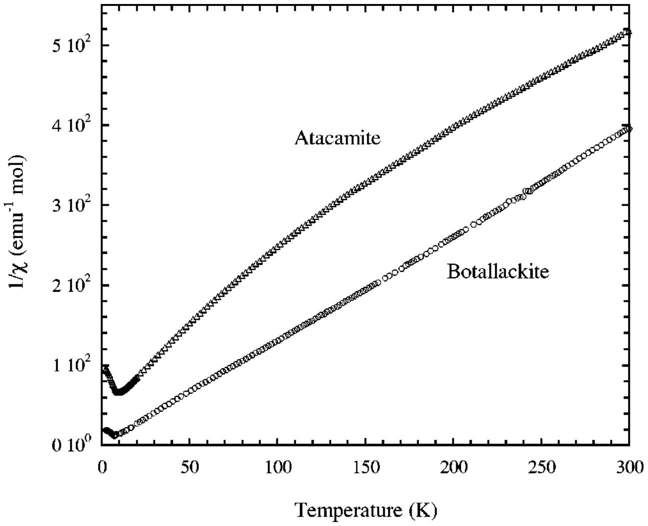

FIG. 7. Temperature dependence of the reciprocal magnetic susceptibility for atacamite and botallackite.

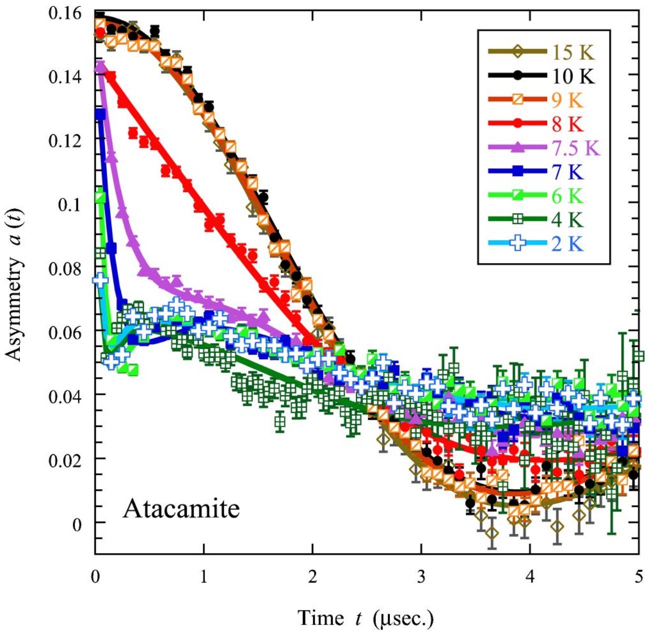

FIG. 8. (Color online) Time evolution of zero-field μSR asymmetry $a(t)$ for atacamite (KEK-MSL). Solid lines for $T > 9$show the Kubo-Toyabe fit with $\sigma = 0.44\ \mu s^{-1}$.

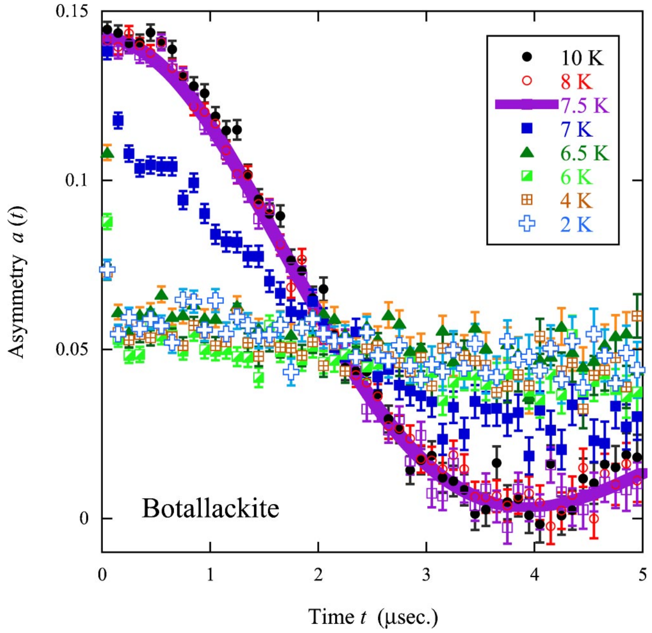

FIG. 9. (Color online) Time evolution of zero-field μSR asymmetry $a(t)$ for botallackite (KEK-MSL). Solid line shows the Kubo-Toyabe fit with σ=0.44 μs^{-1}.

distribution of electron spin field as suggested by the μSR experiment. Contrastingly, in botallackite the bond angle lies in a narrow range of 101°–108°, hence leading to a uniform J.

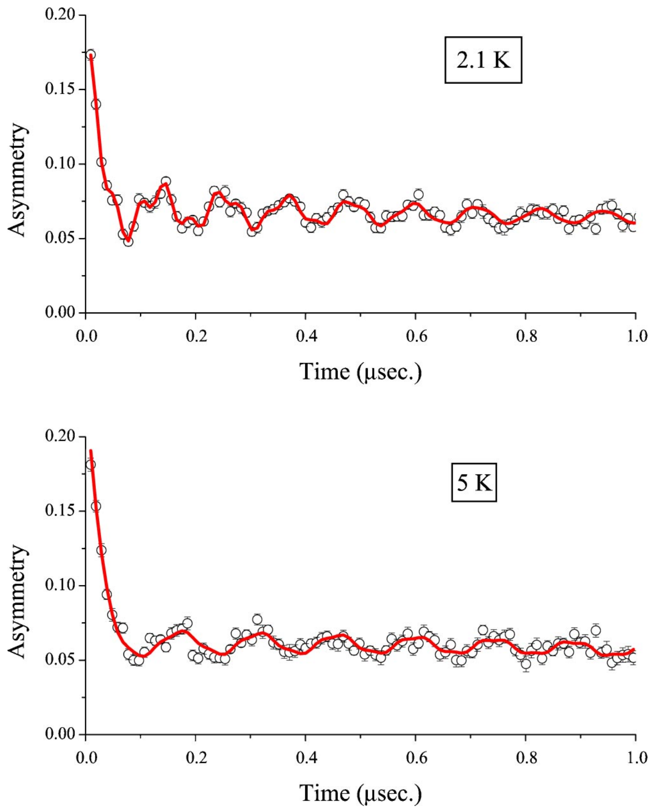

FIG. 10. (Color online) Muon spin rotation seen in the high time resolution zero-field asymmetry spectra (TRIUMF) for botallackite, the solid lines are fitted curves.

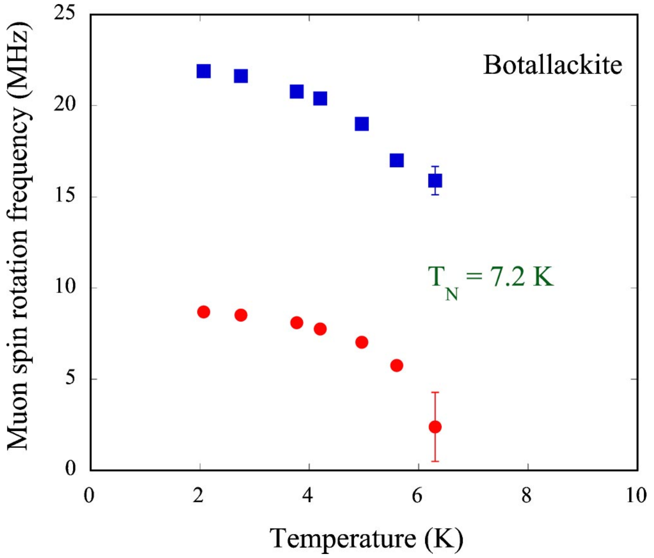

FIG. 11. (Color online) Temperature dependence of the muon spin precession in zero field for botallackite (TRIUMF).

The Cu^{2+} spins in botallackite form a two-dimensional triangle lattice in the b-c plane, which is clearly seen in Fig. 5(b) by eliminating the other atoms. The triangle lattice structure is similar to the layer-structured $Cu_2X(OH)_3$ (X =carboxylate). Antiparallel "up-down" spin arrangement cannot be satisfied for the Cu^{2+} spins in this triangle coordination. However, as is proposed for the botallackite-structured $Cu_2X(OH)_3$,[8,9] a triangular quantum Heisenberg antiferromagnetic lattice with three corner spins pointing to the center can ensure a Neél ground state.

The strong magneto-lattice correlation has been also vividly verified in a simple copper oxide CuO,[18,19] as well in $Cu_{1-x}Li_xO$,[20] by our previous studies on the CuO system. Previous studies on the superexchange coupling in the parent compounds of the high-T_c superconducting cuprates suggested that the superexchange coupling is sensitive to the

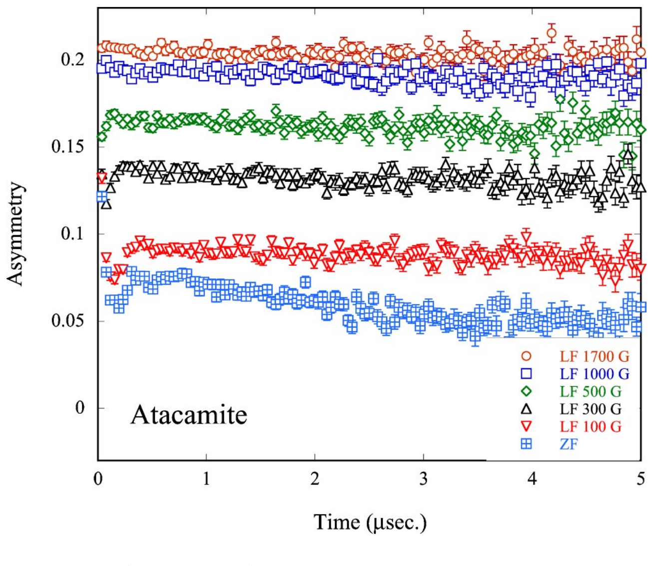

FIG. 12. (Color online) Longitudinal-field μSR asymmetries for atacamite at 2 K (TRIUMF).

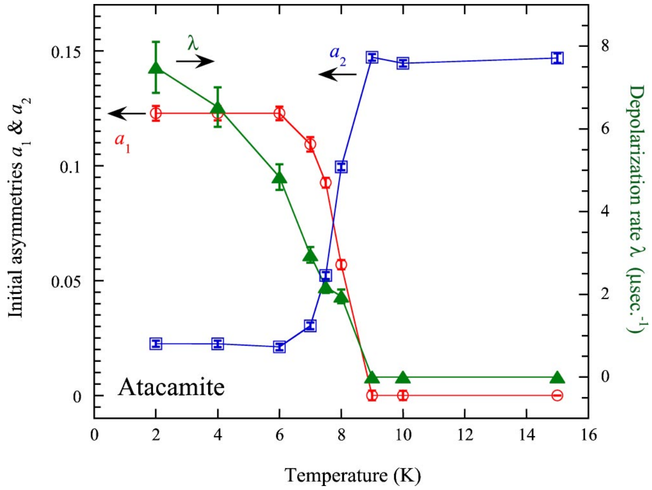

FIG. 13. (Color online) Temperature dependence of the fitted parameters from the ZF-μSR for atacamite.

configuration of the Cu-O bond.[21,22] Therefore, we feel it reasonable to include the natural cuprates into the same copper oxides category in the meaning of strong magneto-lattice correlation. In addition, an updated version of the plot of J versus Cu-O-Cu bond angle as shown in Ref. 22 with the information on botallackite (assuming $J \sim kT_N$) would show a simple power law relation for these copper oxides.

IV. CONCLUSION

In summary, polymorphous atacamite and botallackite are found to be antiferromagnets with $T_N = 9.0$ K and $T_N = 7.2$ K, respectively. A long-range order is verified for botallackite and a disordered ground state is suggested for atacamite. Strong correlation between the magnetic interactions and the crystal structure is revealed. In addition, the discovery of low T_N antiferromagnetism in the natural cuprates may provide a contrasting reference for the high-T_c superconducting cuprates.

ACKNOWLEDGMENTS

This work is supported by a Grant-In-Aid for Scientific Research to X.G.Z. from the Japan Society for the Promotion of Science (JSPS). The synchrotron radiation experiments were performed at the BL02B2 in the SPring-8 with the approval of the Japan Synchrotron Radiation Research Institute (JASRI) (Proposal No. 2003B0365-ND1d-np, 2004A0445-ND1a-np). The μSR experiments are supported by the KEK-MSL and TRIUMF. We are grateful to Prof. Matsushita, Professor Otabe at Kyushu Institute of Technology for facilities in the magnetic susceptibility measurement. We thank Dr. K. Kato at SPring-8 for assistance in the synchrotron x-ray-diffraction experiment.

---

*E-mail address: zheng@cc.saga-u.ac.jp

[1] J. B. Parise and B. G. Hyde, Acta Crystallogr., Sect. C: Cryst. Struct. Commun. **42**, 1277 (1986).
[2] J. Jambor, J. Dutrizac, A. Roberts, J. Grice, and J. Szymanski, Can. Mineral. **34**, 61 (1996); J. Grice, J. Szymanski, and J. Jambor, *ibid.* **34**, 73 (1996).
[3] C. Frondel, Miner. Mag. **29**, 34 (1950).
[4] F. C. Hawthorne, Miner. Mag. **49**, 87 (1985).
[5] M. E. Fleet, Acta Crystallogr., Sect. B: Struct. Crystallogr. Cryst. Chem. **31**, 183 (1975).
[6] W. Mori and K. Yamaguchi, Mol. Cryst. Liq. Cryst. Sci. Technol., Sect. A **274**, 113 (1995).
[7] X. G. Zheng and E. S. Otabe, Solid State Commun. **130**, 107 (2004).
[8] M. A. Girtu, C. M. Wynn, W. Fujita, K. Awaga, and A. J. Epstein, Phys. Rev. B **57**, R11058 (1998).
[9] M. A. Girtu, C. M. Wynn, W. Fujita, K. Awaga, and A. J. Epstein, Phys. Rev. B **61**, 4117 (2000).
[10] W. Fujita and K. Awaga, J. Am. Chem. Soc. **119**, 4563 (1997).
[11] S. Takeda, G. Maruta, K. Terasawa, N. Fukuda, and K. Yamaguchi, Mol. Cryst. Liq. Cryst. Sci. Technol., Sect. A **335**, 723 (1999).
[12] S. Takeda, M. Arai, G. Maruta, and K. Yamaguchi, Mol. Cryst. Liq. Cryst. Sci. Technol., Sect. A **341**, 369 (2000).
[13] S. Yamanaka, T. Sako, and M. Hattori, Chem. Lett. ■**1989**, 1869.
[14] G. Maruta, K. Nishiyama, and S. Takeda, Polyhedron **20**, 1185 (2001).
[15] F. Izumi and T. Ikeda, Mater. Sci. Forum **321–324**, 198 (2000).
[16] R. Kubo and T. Toyabe, *Magnetic Resonance and Relaxation*, R. Blinc, ed. (North-Holland, Amsterdam, 1967), p. 810.
[17] X. G. Zheng, T. Kawae, Y. Kashitani, C. S. Li, N. Tateiwa, K. Takeda, H. Yamada, C. N. Xu, and Y. Ren, Phys. Rev. B **71**, 052409 (2005).
[18] X. G. Zheng *et al.*, J. Phys. Soc. Jpn. **70**, 1054 (2001); Phys. Rev. Lett. **85**, 5170 (2000); J. Appl. Phys. **92**, 2703 (2002).
[19] H. Yamada, X. G. Zheng, Y. Soejima, and M. Kawaminami, Phys. Rev. B **69**, 104104 (2004).
[20] X. G. Zheng, H. Yamada, Daniel J. Scanderbeg, M. B. Maple, and C. N. Xu, Phys. Rev. B **67**, 214516 (2003); X. G. Zheng, Y. Kodama, Kazuya Saito, E. Tanaka, Y. Tomokiyo, H. Yamada, and C. N. Xu, *ibid.* **69**, 094510 (2004).
[21] P. Bourges, H. Casalta, A. S. Ivanov, and D. Petitgrand, Phys. Rev. Lett. **79**, 4906 (1997).
[22] T. Shimizu, T. Matsumoto, A. Goto, T. V. Chandrasekhar Rao, K. Yoshimura, and K. Kosuge, Phys. Rev. B **68**, 224433 (2003).